Supporting Information

Nikitin et al. 10.1073/pnas.1001142107

SI Text

Results and Discussion

Optimization of Particle Conjugation Protocols with Barnase Based on its Enzymatic Activity. As described in the paper, the density of active barnase (DAB) on particles can be quantified using RNAse enzymatic activity of barnase. Here we provide an example of conjugation protocol optimization for barnase and 500 nm MP (MagSense). The dependence of DAB on N-(3-Dimethylaminopropyl)-N′-ethylcarbodiimide (EDC) amount used to activate the carboxyl groups on the particles surface was studied. Fig. S2 presents the data for two MP samples: (green)—MP activated by 40-fold excess of EDC over MP (w/w); (red)—activated by 10-fold excess. The rest of the conjugation protocol was similar. After performing the enzymatic activity study described in our previous work (1), we calculated the DAB for the described particles based on calibration (Fig. S2, *Blue*) using molecular barnase not conjugated with any particles, and control raw MP not conjugated with barnase (*Black*). The DAB value for the MP activated with 40-fold excess of EDC was one active barnase/300 nm^2 (17 nm between two active molecules), whereas for the 10-fold excess of EDC sample the DAB value was one active barnase/2000 nm^2 (44 nm between two active molecules). Therefore, 40-fold excess of EDC was used for these particles. Using the same process, the conjugation was optimized for other particles involved in building superstructures as described in the main text of the paper. The enzymatic activity of barnase can be also used to estimate the density of active barstar that inhibits barnase's activity.

Dependence of the Size Dispersion of the Superstructures on the Ratio Between Modules. In the experiment with the assembly of superstructures by mixing two modules at different ratios, the size of the structures as well as its dispersion depended on the ratio between smaller and larder modules. Explanation for size dependence is given in the main text. Here we describe the main reasons for the dependence of the size dispersion on the ratio between the modules. For the right point of Fig. 5 where the structures could be represented as the unique module covered be a shielding layer of the other modules, the major part of roughly 10% size dispersion of the structures can be attributed to the size variation of modules, i.e., the particles of which they consist. Almost 40% dispersion for the points in the midrange is due to the assembly process. For the left point of Fig. 5, the situation is slightly different: the number of smaller modules connected with the larger module determines the dispersion of the structure sizes. However, because we used 53 nm particles as the smaller modules (size is about 10% of that of the 500 nm larger modules), the dispersion turned out to be around 15%, similar to the size dispersion of the larger modules.

1. Edelweiss E et al. (2008) Barnase as a new therapeutic agent triggering apoptosis in human cancer cells. *PLoS One* 3:e2434.

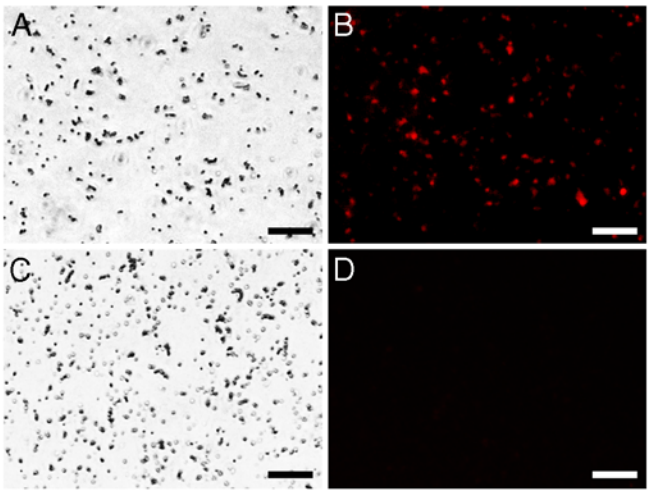

Fig. S1. Photographs of the assembled bifunctional structures. (*A* and *B*) {[MP-Bn] + [Pink-Bs]} structures assembled by mixing modules of 500 nm magnetic particles conjugated with barnase, and 53 nm fluorescent polystyrene particles conjugated with barstar after magnetic washing of unbound fluorescent particles. (*C* and *D*) control experiments: {[MP-BSA] + [Pink-Bs]} structures assembled by mixing modules of the same magnetic particles conjugated with BSA and the same polystyrene particles conjugated with barstar after magnetic washing of unbound fluorescent particles. (*A* and *C*) bright-field pictures, (*B* and *D*) pictures made with excitation of fluorophores. The control structures demonstrate no or much weaker fluorescence. (Scale bar: 10 μm.)

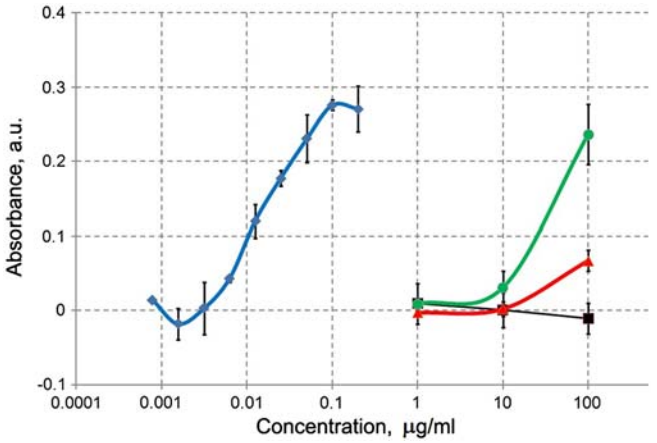

Fig. S2. Optimization of the conjugation protocol of 500 nm MP (MagSense) with barnase by DAB estimation on the particles using RNAse enzymatic activity of barnase: (*Blue Diamonds*)—calibration curve of pure molecular barnase, (*Black Squares*)—raw MP, not conjugated with barnase, (*Red Triangles*)—MP activated by 10-fold excess of EDC during conjugation, (*Green Circles*)—MP activated by 40-fold excess of EDC. Error bars represent standard deviation based on two experiments.

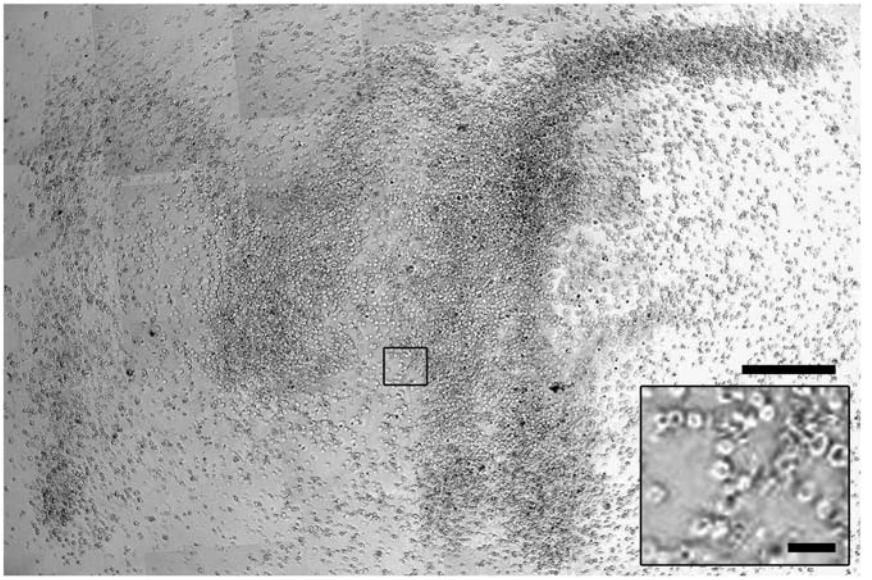

Fig. S3. High-resolution version of Fig. 3*B*. Magnetic field-guided inscription of MF-letters layout, standing for MultiFunctional, with cancer cells labeled by trifunctional superstructures. A drop of human ovarian cancer (SKOV-3) cell suspension labeled with the assembled trifunctional structures was put on the surface of a glass slip located above the ferromagnetic foil. The applied magnetic field magnetized the foil to produce the magnetic gradients that dragged the cells labeled with magnetic structures toward the contour of letters MF. The bright-field image made by digital combination of multiple overlapping photos at 100x magnification into a single photograph to visualize individual cells over a large field of view. The inset of the figure shows approximately 30 cells in the area of view. (Scale bar: 0.5 mm.) *Inset*: 50 μm.

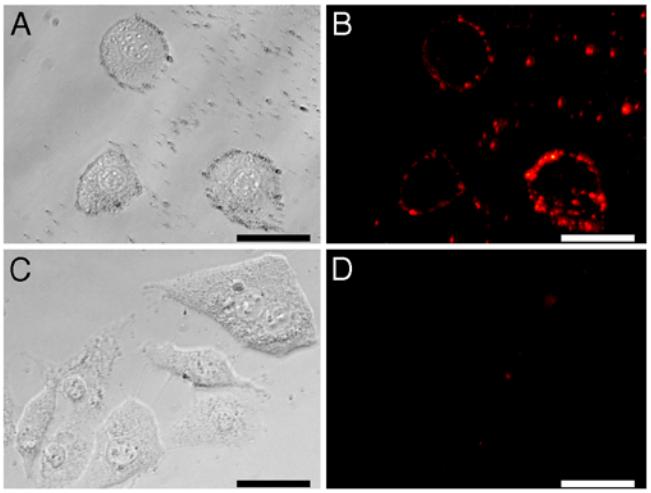

Fig. S4. Labeling the SKOV-3 cells with the assembled trifunctional structures {[MP-Bn] + [QD-Bs] + [4D5scFv-Bn]} (*A* and *B*) and control structures {[MP-BSA] + [QD-Bs] + [4D5scFv-Bn]} (*C* and *D*). (*A* and *C*) bright-field photos of the cells in fluorescent microscope; (*B* and *D*) fluorescence images of the same cells with UV excitation. (Scale bar: 17 μm.)

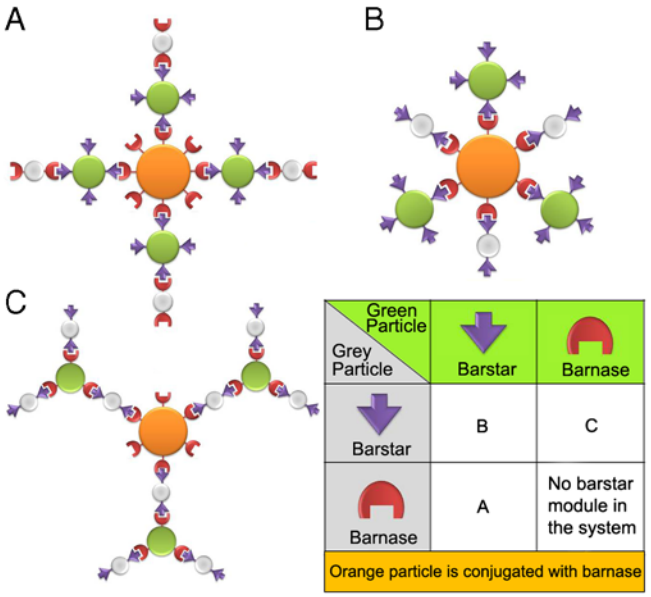

Fig. S5. Two-dimensional representation of Fig. 4. Possible variants for assembling of three particles into a superstructure by the protein-assisted nanoassembler method. Correspondence of different combinations of BBS proteins conjugated with the green and gray particles and the structure number (*A*, *B*, *C*) is shown in the table. Barnase is chosen as the protein conjugated with the core orange particle.